DIMES CONTRIBUTIONS TO PMI UNDERSTANDING

by
C.P.C. WONG, D.G. WHYTE, R. BASTASZ,
W. WAMPLER, J.N. BROOKS, T.E. EVANS, W.P. WEST,
J. WHALEY, R. DOERNER, J.G. WATKINS, J.P. ALLAIN,
A. HASSANEIN, and D.L. RUDAKOV

DISCLAIMER

DIMES CONTRIBUTIONS TO PMI UNDERSTANDING

by

C.P.C. WONG, D.G. WHYTE,[†] R. BASTASZ,[£]
W. WAMPLER,[§] J.N. BROOKS,[¶] T.E. EVANS, W.P. WEST,
J. WHALEY,[£] R. DOERNER,[*] J.G. WATKINS,[§] J.P. ALLAIN,[¶]
A. HASSANEIN,[¶] and D.L. RUDAKOV[*]

[†]University of Wisconsin, Madison, Wisconsin
[£]Sandia National Laboratory, Livermore, California
[§] Sandia National Laboratory, Albuquerque, New Mexico
[¶]Argonne National Laboratory, Argonne, Illinois
[*]University of California, San Diego, California

DiMES Contributions to PMI Understanding

C.P.C. Wong,[a] D. G. Whyte,[b] R. Bastasz,[c] W. Wampler,[d] J. N. Brooks,[e] T.E. Evans,[a] W.P. West,[a] J. Whaley,[c]
R. Doerner,[f] J. Watkins,[d] J.P. Allain,[e] A. Hassanein,[e] D. Rudakov[f]

[a]*General Atomics, P.O.Box 85608, San Diego, CA, 92186-5608*
Phone: 858-455-4258, fax: 858-455-2838, wongc@fusion.gat.com
[b]*University of Wisconsin, Madison, Wisconsin*
[c]*Sandia National Laboratory, Livermore, CA*
[d] *Sandia National Laboratory, Albuquerque, NM*
[e]*Argonne National Laboratory, Argonne, IL*
[f]*University of California, San Diego, CA*

***Abstract*.** **The Divertor Materials Evaluation System (DiMES) program at General Atomics has been using a sample changer mechanism to expose different plasma-facing materials to the lower divertor of DIII–D to study integrated plasma materials interaction effects in a tokamak and to benchmark modeling codes. We found that for carbon divertor plates, a detached plasma eliminates net erosion in DIII–D. A spectroscopic study of chemical sputtering indicated the potential improvement of erosion arising from the aging of the first wall material. We also found the importance of the carbon source from the first wall of DIII–D. When lithium was exposed at the divertor we found significant and complicated MHD interactions between the scrape-off layer current in a tokamak and the conducting liquid. This paper is a report on what we have learned and what we plan to do in response to the needs for the plasma facing components (PFC) design for advanced tokamak machines like ITER. Our plan for the study of liquid surface interaction with the plasma will also be presented.**

I. INTRODUCTION

For advanced tokamak experiments and power reactors, divertor surface and chamber wall material erosion and redeposition will have critical impacts on the performance of the plasma due to impurities transport, the lifetime of the plasma facing components and the migration and inventory of tritium. The Divertor Materials Evaluation System [1] in DIII–D [2] provides measured data of suitable surface materials for advanced tokamak devices like ITER and fusion power reactors. Material samples can be inserted into the lower divertor of DIII–D and exposed to different plasma discharges. Net material erosion and redeposition can be measured and results can be used to benchmark modeling codes. This paper summarizes the significant contributions that the DiMES program has provided to the area of plasma material interaction (PMI) and the plan for the next phase of research with in-situ measurements.

II. DiMES EXPERIMENT IN DIII–D

A. *The DiMES Team*

The DiMES program is supported by a national team; members are from ANL, SNL-Livermore, SNL-Albuquerque, UCSD, UW, UIUC and DIII–D. The DIII–D DiMES team provides the coordination of sample exposure and the collection and distribution of core plasma and scrape-off layer (SOL) plasma parameters.

B. *DiMES Experiment*

ATJ graphite samples with diameter of 4.8 cm and polished to 0.25 μm finish on the plasma side, some with a depth marker of silicon implanted at ~300 nm below the surface using a 200 kV ion beam, can be inserted into the lower divertor of DIII–D (Fig.1). Metal films 100 nm thick and solid lithium foils are deposited on the graphite surface via electron beam evaporation deposition and physically applied, respectively. After the desired plasma conditions have been obtained, the sample is inserted and exposed to selected single plasma conditions. This is critical in that the erosion results obtained are related to the particular discharge. We have exposed samples to various plasma regimes: high and low beam heating discharges, edge localized mode (ELMs) and disruptions. Several exposures were used to accumulate exposure times of 4–20 s.
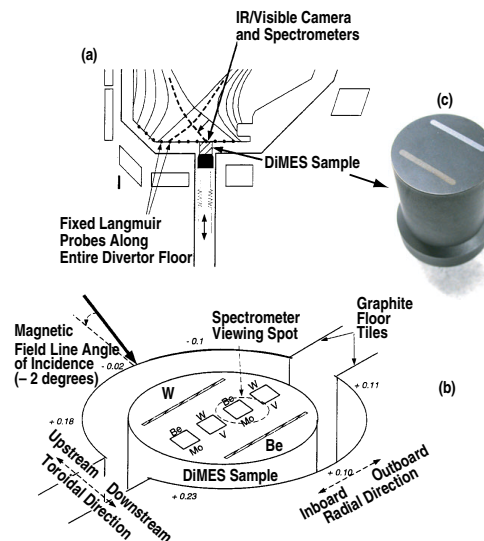
Fig. 1. (a) Poloidal cross-section of DiMES and corresponding lower divertor diagnostics. (b) DiMES sample, metallic films and surrounding graphite tile geometry, with indication of relative height of the tiles and alignment in mm. The gap between the sample and the tiles is exaggerated for viewing clarity. (c) Picture of a DiMES sample with Be and W coatings.

C. *DIII–D Experiment*

The DIII–D tokamak was converted to 100% graphite coverage for all plasma-facing surfaces in the fall of 1992, and with a divertor configuration [2]. Carbon is the only major

component as an intrinsic impurity, even with frequent boronizations, with a concentration of 1-2% [3]. Since carbon has been selected as one of the divertor surface materials for ITER because of its tolerance to transient heating such as from disruptions, many of our experimental results are relevant to the ITER design in the areas of surface material erosion and re-deposition and tritium uptake. The latter is represented by deuterium in DIII–D. The oxygen concentration of the DIII–D core plasma is 0.1-0.2%. Other typical plasma parameters of interest for our experiments are: D_2 gas, plasma current I_p=1.35–1.4 MA, magnetic field strength B_T=2.1T, central plasma Z_{eff}=1.5, and neutral beam injected power from 2.5 to 7 MW, with corresponding maximum heat flux of ~0.7-2 MW/m^2. The graphite floor tile temperature typically reaches ~50°C during operations.

D. Diagnostics and erosion/redeposition measurements

The DIII–D tokamak has a very large array of divertor diagnostics to characterize plasma conditions causing the measured erosion: fixed Langmuir probes measure edge electron temperature, T_e and density, n_e at the divertor surface; EFIT is a magnetic re-construction code to provide magnetic field configuration; Divertor Thomson scattering provides n_e, T_e data (including accurate measurement of very low T_e in detached plasma); infrared thermography (IRTV) for surface temperature; visible camera equipped with interference filters to record carbon line emission and also to view the lower divertor floor and DiMES sample; Thomson scattering to measure upstream density and temperature; and charge exchange recombination spectroscopy to measure impurity concentrations in the core plasma [4]. For the absolute measurement of net erosion, the Rutherford back scattering (RBS) analysis is conducted using a beam of 2 MeV He$^+$ to detect the effective depth of a pre-exposure implanted silicon depth marker. Precision of the depth measurements is ±10 nm. Nuclear Reaction Analysis (NRA) is used to measure the amount of transported Be to the surrounding carbon surface. Retention of deuterium in the samples is mapped by NRA from the d(^{3}He, p)α nuclear reaction with a 700 keV ^{3}He analysis beam [5]. The experimental method for performing the DiMES experiment and measuring net erosion with DiMES has been previously described [4,6].

III. SOLID MATERIALS RESULTS

A. Physical sputtering of carbon

Systematic experiments were performed to study the erosion of carbon under different plasma discharge conditions and to make comparisons with modeling code results. Typical divertor plasma has peak T_e~40 eV, n_e=4x10^{19}/m^3, ion flux, Γ_i=3x10^{22}/m^2 s, B_T=2.1 T, magnetic field pitch ~2.5°, I_p=1.5 MA, neutral beam power=2.5 MW, and corresponding heat flux peaked at 0.70 MW/m^2. Measured C erosion rate for carbon target, attached divertors at the outer strike point (OSP) is ~4 nm/s, which translates to ~12 cm/exposure-year [6, 7]. This erosion rate would not be acceptable for steady state operation when heat transfer and other factors are taken into consideration. In comparison, under similar plasma conditions, the erosion rates for Be and W are ~0.9 and ~0.1 nm/s, respectively. However, the erosion of non-carbon species is complicated by the dominance of carbon in the divertor plasma. The maximum net erosion rate for carbon, which occurs near the separatrix, increased to 16 nm/s when the incident heat flux was increased to 2 MW/m^2, which was obtained by

increasing the neutral beam power to 7 MW. Scaling studies show that the erosion rate of materials increases with heat flux in the attached plasma. Comparison of the measured carbon erosion and redeposition using the REDEP code show good agreement for both the absolute net erosion rate and its spatial variation [8,9] as shown in Fig. 2. The ratios of net to gross erosion for the sputtered carbon indicate a prompt redeposition efficiency of ≥ 80-85% near the OSP in both the model and experiment. Correctness of the assumptions made in the modeling was also confirmed by sensitivity studies by varying the oxygen content, increase of self-sputtering, elimination of chemical sputtering, change in self-sputtering and normal incidence of D$^+$ and D^0. It was shown that the dominating effects are self-sputtering and angle of incidence to the sample surface [10].

B. Detached plasma

Detached divertor plasma is a plasma condition characterized by lower temperature (T_e<2 eV), high density (n_e > 10^{20} m^{-3}) and high particle flux (Γ_i ~ 10^{23}/m^{2}s). Semi-detachment is the operation state of the ITER divertor in order to restrict peak heat flux to ~10 MW/m^2. For cold plasma temperatures and incident particle energies measured in detached plasma, chemical sputtering is the only expected source of erosion (e.g. Y_{chem} ≤ 10^{-2} >> $Y_{physical}$ ~0). We found that the heat flux is reduced by a factor of 5-10 at the OSP compared to an attached divertor with the same input power. Molecular spectroscopy indicates an upper limit of Y≤0.1% for the chemical sputtering yield. For these experiments, OSP detachments were obtained by controlled injection of deuterium, neon or argon gas, the latter two which cool the plasma edge by radiation [11,12,13]. However, a high rate of carbon deposition ~3 cm/burn-year could be extrapolated, with the corresponding hydrogenic codeposition rate > 1 kg/m^2/burn-year [14]. It is also noted that when Ne was used as the detachment gas, the rate of carbon net erosion at the outer strike point was very high (~15 nm/s), in contrast to the absence of erosion from plasma detached by deuterium injection [13]. A complete explanation of this somewhat surprising result is not yet available.

Another important result in detachment was that, despite the reduction in divertor erosion in DIII–D with detachment and with insignificant erosion from both physical and chemical sputtering, no significant reduction is found in the core plasma carbon density [7,12]. Recent observations have shown that the main-wall was the controlling location for the core carbon impurity content [14].

C. Chemical sputtering

A comprehensive spectroscopic survey was performed to assess chemical sputtering over a ten year period in DIII–D [15]. Newly installed virgin graphite tiles in 1992 were found to have a chemical erosion yield, Y_{chem} ≤ 3-5%, consistent with both laboratory results and similar experiments in other tokamaks. However, the average Y_{chem} measured in the DIII–D lower divertor outer strikepoint region decreased approximately a factor of five between 1992 (shot # 75,000) and 2000 (shot # > 100,000) as shown in Fig. 3. The presumed cause of this reduction is the cumulative effect of >30 wall-conditioning boronizations and 10^5 s of plasma exposure, although the relative importance of these two mechanisms is unknown. Furthermore, in detached plasma the absence of
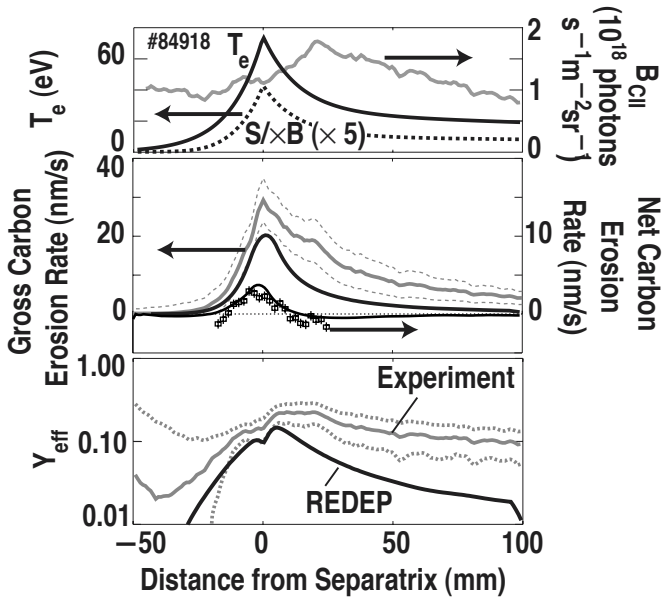
Fig. 2. Radial profiles near outer strike point in low power attached plasma. (Top) Measured plasma temperature and CII brightness and calculated ionization/photon ratio (S/XB). (Middle) Measured (gray line and points) and REDEP predicted (dark line) gross (ELM-free case) and net (ELMy case) carbon erosion rates. (Bottom) Measured and REDEP predicted effective sputtering yield.

upper limit on the chemical sputtering yield ~0.1% [7], which shows that it is also not a source of carbon from later shots. Detailed spectroscopic analysis of C-I emission suggested that the source of carbon was not dominated by ELMs, nor chemical sputtering in detachment, but more likely from carbon ions from the core and SOL transporting into the cold dense plasma and recombining to neutral state. This also can explain the source of deposited carbon at the inboard and private region [14]. This explanation was also speculated from earlier work [16].

The source of carbon to the core could most likely be from the chamber wall. This indicates also the necessity to coordinate the assessment with the study on the phenomena of intermittent convection plasma transport [17], which could have significant impact to the enhancement of chamber wall erosion.

D. General erosion and redeposition pattern

Between March 1989 and December 1989, 12 selected lower divertor tiles were exposed to 1700 discharges in DIII–D. We found inboard net deposition and outboard net erosion. Carbon net deposition rates vary across the divertor floor, being highest near the strike points (~3-5 cm/burn-year), and lowest at the private-flux and outer SOL ≤ 1 cm/burn-year as shown in Fig. 4 Corresponding patterns can be noted on the near surface deuterium areal density. Similar poloidal patterns of divertor deuterium areal distribution of the ASDEX Upgrade, JET and DIII–D tokamaks have also indicated that the outer divertor strike point undergoes net erosion and the inner divertor is a region of net deposition [18]. The quantities of deposition are quite similar, despite their differences in geometry, size, and plasma facing materials, indicating the commonality of the phenomena of carbon erosion and redeposition from tokamaks.
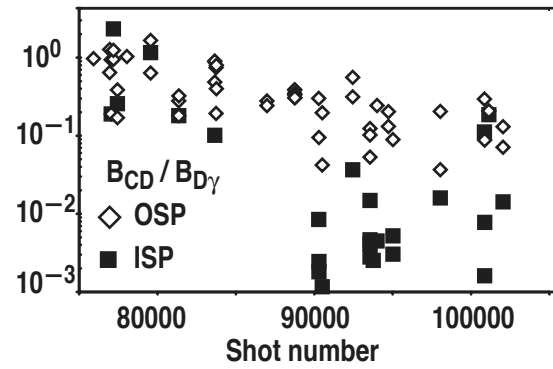

Fig. 3. Spectroscopy of divertor carbon in DIII–D from 1992 (shot # 75,000) to 2000 (shot # 100,000). ELMing H–mode confinement regime with attached outer divertor plasma unless otherwise noted. $B_{CD}/B_{D\gamma}Y_{chem}$ at OSP region.
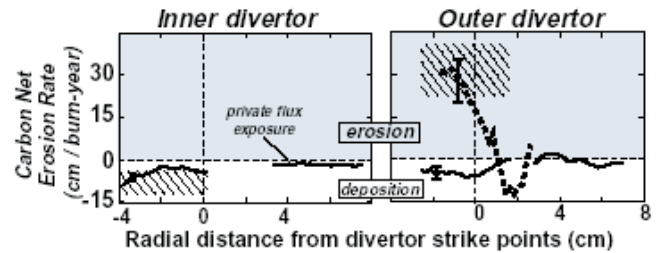

Fig. 4. Summary of lower divertor erosion and redeposition rates of DIII–D. The lines show a comparison of the attached (dashed lines) and detached (solid lines) divertors at 7 MW neutral beam heating measured with DiMES sample probes. The hatched areas indicate height measurements on DIII–D tiles exposed for nine months. [1] Net redeposition is plotted as negative net erosion.

E. Impacts from first wall and plasma operation

Based on the measurement of physical sputtering, the near elimination of physical sputtering via detached plasma and the insignificant contribution from chemical sputtering, we concluded that the divertor is not the dominant source location of impurities found in the core plasma, i.e. the main chamber wall should be relatively as important [16]. However the chamber impurities transport does not behave in a straight forward manner, the core impurity transport seem to adjust such that the core contamination varies non-linearly with the source rate of impurity at the plasma-wall interface as supported by the UEDGE multi-fluid modeling code [19].

F. Leading Edge effect

A DiMES sample with a 0.7 mm vertical lip above the divertor floor was exposed to the outer strike point (OSP) of an ELMing H–mode plasma, with a divertor surface heat flux of ~2 MW/m^2. Correspondingly, the parallel heat flux to the vertical lip was ~50 MW/m^2, and the thermal analysis shows a temperature > 2300°C [4]. Extremely high erosion/ablation rates were measured from the leading edge, causing significant local carbon influx into the divertor plasma.

G. ELMs

A sample was exposed to an ELMing H–mode with peak heat flux of 0.8 MW/m^2 in order to compare the carbon erosion with a case without ELMs with the same average

power flux. The ELMs have a typical energy of 0.02-0.04 MJ (or a power density of < 10 MW/m^2) per ELM in DIII–D. For this exposure, the duty cycle of the ELMs is 3%, given by an ELM frequency of 60 Hz and an average ELM duration of 0.5 ms. We found that the carbon net erosion rate was not affected by the presence or lack of ELMs. (It must be noted that the energy density of ELMs on DIII–D cannot produce ablation, which is considered to be the major contributor to carbon erosion in ITER-like ELMs). Modeling of the net erosion during ELMs agreed with experimental results: the large density associated with the ELM caused extremely high local redeposition efficiency for eroded carbon during ELM. One should note that the situation would be quite different with ITER when the estimated ELMing energy is 8-20 MJ and with similar deposition time [8].

H. Disruption

A specially designed DiMES sample with a slotted particle analyzer was used to measure the ion energy distribution at the divertor strike point during Ar-induced disruptions in DIII–D, with the implanted D atoms collected in a silicon wafer collector. We found that the incident ion energy was approximately 100 eV at normal incidence and decreased slightly at oblique angles [20]. In the case of the density limit disruption, the peak heat flux to the floor was < 100 MW/m^2 [21].

I. Erosion/codeposition of different materials

Different multi-materials samples were exposed to ELM free and ELMing discharges: Be, W, Mo, V thin metal films were deposited on Si depth-marked graphite samples. Net erosion and deuterium retention were measured [4,5,22]. This choice of material was in response to the selection of Be, W and C as the chamber and divertor wall material for ITER [23] and fusion power reactors. For modeling purposes the net erosion rate is calculated by considering the interaction of hydrogen isotope, trace element sputtering, self-sputtering, and impurity transport in the sheath, near surface region, SOL, and the core plasma. For DIII–D, the resulting absolute erosion is less than that for pure metal due to the effects of carbon overlay or mixture. This was noted for most metal films [8]. The experimental data shows a decrease of erosion rate as a function of atomic number A, which can be approximated by sputtering yield Y proportional to $e^{-A/77}$ [4]. The prediction of the yield for the V-coating is the most uncertain; due to the lack of adequate atomic data. Relatively, W has the lowest erosion rate, which is about ~100 times lower than carbon. W near surface erosion/deposition and particle transport were inferred from transported and deposited film material measured by RBS, since its e-folding distance is ~2 mm [6,24]. Furthermore, we found that the erosion of the W-film was dominated by arcing. This was determined to occur during quiescent plasma exposure. The arcs predominately originated at the small surface defects, a result expected from the theory of unipolar arcing. We hope to better quantify the effect of arcing on W divertor surface with future experiments since frequent arcing could contribute significantly to erosion. Under the high particle flux found in a tokamak divertor ($>10^{22}$ /m^{2}s) we have found that all surfaces reach their surface hydrogenic saturation point after only ~0.1 s. The saturated retention of deuterium of these metal coatings was also measured and agrees well with results from laboratory experiments [5,9]. All materials had H saturation fluence within factor of four of the carbon materials.

J. Future work

For the next phase of solid surface material research we will be making use of our capability of in-situ measurements. We will be inserting solid state hydrogen micro-sensors to quantify the flux and energy from charge exchange neutrals and use micro-balances to provide *in-situ* measurement of erosion and redeposition. To address the question of chamber wall erosion, we have begun to perform upper single null discharge experiments to simulate material erosion at the first wall. We are using the disruption energy deposition from DIII–D to simulate the ELMing effect for ITER on carbon surfaces. We will also focus our attention to chemical sputtering by controlling the sample surface temperature to study its impacts on chemical sputtering for virgin and boronized graphite. We will continue to characterize the coating from wall conditioning (e.g., boronization) in DIII–D. We will also continue to support the development of advanced diagnostics and the study of sheath physics.

IV. LIQUID/LITHIUM WALL RESULTS

An innovative approach for the choice of plasma facing material is lithium due to its ability to control net surface erosion, since it can be replenished and high surface heat flux can be removed with lithium circulation. Due to its affinity for hydrogen, lithium can be used to pump/getter hydrogenic fuel. This could also have favorable impacts on plasma performance by achieving a low recycling edge [25]. Several sets of experiments with solid lithium discs (2.54 cm in diameter and ~ 1.3 mm thick) were exposed to the divertor plasma of the DIII–D with results as shown in Fig. 5. The experiments revealed important information on the application of liquid lithium, and conducting liquid metals in general, as a plasma-facing surface in a tokamak divertor,

A. Cleanliness

We learned that a contaminated lithium surface from exposure to air, forming oxide and nitride, would strongly impact the surface interaction with the plasma. Divertor plasma strikepoint exposure was found to clean and condition the lithium surface. The technique can only be used to remove a slightly contaminating layer resulting from exposure to the air.

B. Sputtering

The sputtering rate and transport of lithium from the divertor was found to be acceptable. The sputtering yield of solid lithium ($<10\%$ for T_e~20 eV) intrinsically includes the effects of self-sputtering and oblique incidence important in divertor erosion. The sputtered lithium is ionized in a short distance from the divertor and promptly redeposited. Experiments and modeling show the sputtered lithium is well shielded by the divertor plasma [26].

C. ELMs and locked modes

Due to the low melting point of lithium at 180°C, we found that the solid lithium disc can easily be melted by high power and ELMing discharges, and by disruptions. The behavior of the liquefied lithium was dominated by its macroscopic movement and injection into the plasma caused by JxB MHD forces. The JxB MHD motion was observed to be caused by both non-disruptive plasma MHD events even when exposed to quiescent L–mode plasmas with minimal plasma-induced instability. The plasma MHD events (ELMs and locked modes) were found to provide simultaneously the energy to

melt the lithium and the transiently high SOL currents to cause the JxB motion as shown in Fig. 6(b) [27].

D. Low power L–mode and MHD effect

We examined a case where tokamak plasma MHD events were intentionally avoided by exposing Li–DiMES to a series of non-ELMing quiescent, low power (P_{NB}<1 MW) L–mode discharges. The heating from the plasma strike point was carefully controlled. When the local heat flux was increased from ~0.4 MW/m^2 to ~0.7 MW/m^2 and after 2 s of exposure the lithium movement was recorded by imaging. After ~3.4 s of discharge, the molten lithium sample became unstable and was macroscopically injected into the divertor plasma and eventually disrupted the discharge due to radiative collapse, with macroscopic removal of lithium resulting on what was left on the DiMES sample as shown in Fig. 6(c). The macroscopic
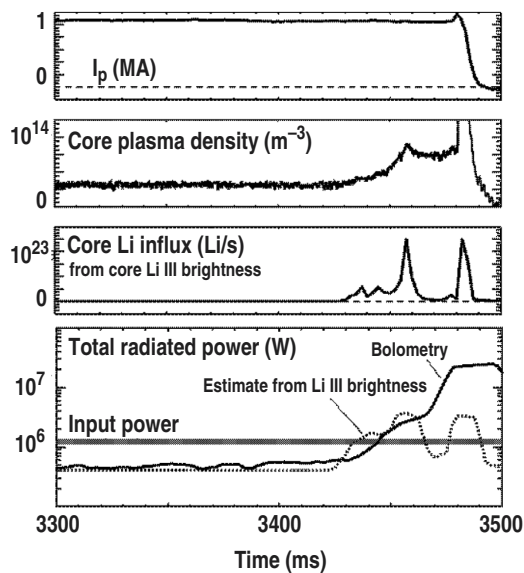

Fig. 5. Core plasma parameters as a function of time for L–mode discharge with OSP ~30 mm inboard of the Li–DiMES. The disruption is caused by injection of lithium at ~3420 ms and again at ~3480 ms, with an increase of core density and radiative power.

removal of lithium from the small sample (comprising <1/1000th of the wetted divertor area) led to measurable contamination of the core plasma by lithium. The quantity of injected lithium was sufficient to cause a radiation limit disruption. A complete explanation of the lithium movement is not yet available. One of the difficulties in explaining this vertical injection is that the injection itself is highly perturbative to the local plasma conditions. 3-D MHD modeling is being used to simulate the result. We believe that surface stability and JxB MHD motion are the most critical issues with regard to liquid-metal divertor surfaces. A new Li DiMES experiment that can be heated to melt the lithium and with coating on the Li–cups to assure surface wetting, has been designed to study in more detail the spatial and temporal evolution of the parallel current in order to understand the convoluted development of the JxB effect and the corresponding movement of the liquid lithium. We will be aiming for the possibility of mitigating the vertical injection of lithium into the plasma core.
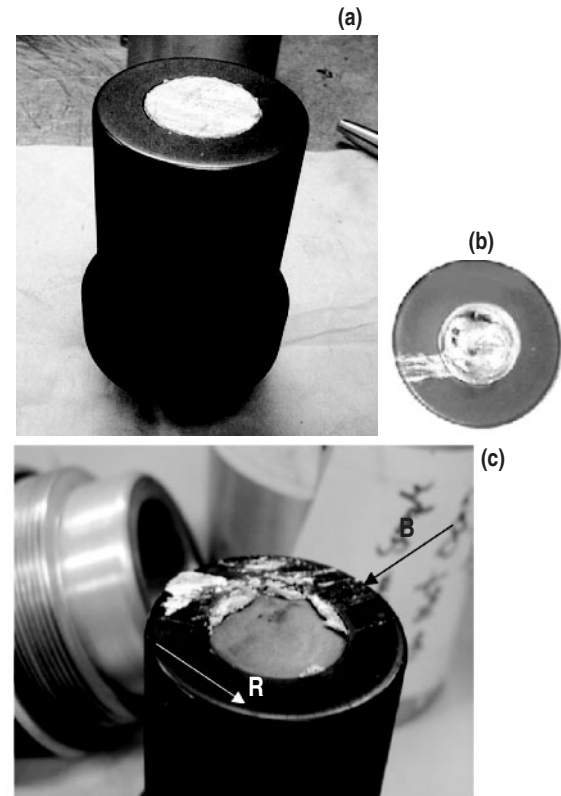

Fig. 6. (a) DiMES sample photograph before exposure, (b) *ex-situ* photograph of lithium splash pattern on stainless-steel cup after exposure to near locked-mode discharge, showing lithium ejection by JxB forces. Magnetic field (B) and tile current density J_z direction indicated, (c) *ex-situ* photograph of lithium after vertical injection that caused a density limit disruption, with removal of most of the lithium due to JxB effect. (Detailed cause of the disruptive event still under investigation.)

V. DISCUSSION

DiMES experiments have shown surface material erosion and redeposition behavior from the divertor and the first wall of a tokamak chamber under different plasma operating regimes. Unfortunately, even with reduced erosion at the divertor, the overall carbon erosion and redeposition rates from a carbon wall machine would still be uncertain. The carbon erosion from the divertor can also lead to significant tritium inventory concerns from the re-deposited carbon for a device like ITER. In a carbon background plasma, a W surface would have a maximum erosion rate ~100 times lower than carbon. Therefore, a W surface could be a good candidate plasma surface material if the effect of microscopic damage from energetic helium ions can be eliminated [28,29] and surface melting avoided. We have learned that the details of chemical and physical erosion would be impacted by possible aging of the wall from repeated wall conditioning and plasma operation. The last observation shows the importance of performing integrated exposure experiments in an operating tokamak that can provide information on the aging process with repeated wall conditioning and plasma discharges and help to identify the necessary coating or aging sequence for advanced devices including ITER. When the effects from charged particles and neutron irradiation are taken into consideration, one can foresee the need for the Components Testing Facility (CTF) [30], as a necessary vehicle to also provide the necessary material surface evolution of a steady state D-T device.

VI. Conclusions

The DiMES program has made significant contributions to the understanding of PMI for tokamak machines. With the carbon background plasma, integrated information on physical sputtering for different relevant materials has been obtained under different regimes of plasma operation. Detached divertor has shown to reduce the maximum erosion rate at the divertor, but the redeposition could still be unacceptably high even for a pulse machine like ITER. The additional eroded material source could be from the first wall. The full story on the lack of chemical sputtering in DIII–D is not understood, but it shows that significant impacts to plasma edge properties could be from the aging of the first wall material. When conducting liquid is present, we found that, due to the presence of parallel current in a tokamak, significant MHD interaction should be expected. This applies to the situation of liquid surface material and the liquid material generated from melting. Results from DiMES not only do indicate the importance of the area of PMI but also show the need for integrated investigations in an advanced tokamak in order to identify the best first wall material solution for the long burn and steady state devices. For our next phase of work we will be making use of the *in-situ* measurement and control capability of the DiMES system.

Acknowledgment

References

[1] C.P.C. Wong, R. Junge, R.D. Phelps et al., "Divertor materials evaluation system at DIII–D," J. Nucl. Mat., **196-198** (1992) 871-875

[2] J.L. Luxon, "A design retrospective of the DIII–D tokamak," Nucl. Fusion **42** (2002) 614.

[3] D.G. Whyte, M.R. Wade, D.F. Finkenthal et al., "Measurement and verification of Z_{eff} radial profiles using charge exchange recombination spectroscopy on DIII–D," Nuclear Fusion, Vol.**38**, No. 3 (1997)

[4] D.R. Whyte, J.N. Brooks, C.P.C. Wong et al., "DiMES divertor erosion experiments on DIII–D," J. Nucl. Mat. **241-243** (1997) 660-665.

[5] W.R. Wampler, R. Bastasz, D. Buchenauer, "Erosion and deposition of metals and carbon in the DIII–D divertor," J. Nucl. Mat., **233-237** (1996) 791-797.

[6] R. Bastasz, W.R. Wampler and J.W. Cuthbertson et al., "Measurements of carbon and tungsten erosion/deposition in the DIII–D divertor, J. Nucl. Mat. **220-222** (1995) 310-314.

[7] D.G. Whyte, R. Bastasz, J. N.Brooks et al., "Divertor erosion in DIII–D", J. of Nucl. Mat. **266-269** (1999) 67-74

[8] J.N. Brooks, D.G. Whyte, "Modelling and analysis of DIII–D/DiMES sputtered impurity transport experiments," Nucl. Fusion, Vol. **39**, No 4, 1999.

[9] J.N. Brooks and D.G. Whyte, "Modelling and analysis of DIII–D/DiMES sputtered impurity transport experiements," Nucl. Fusion, Vol. **39**, No.4, 1999.

[10] J.N. Brooks, "Transport calculations of chemically sputtered carbon near a plasma divertor surface, rep. ANL/FPP/TM-259, Argonne National Lab., IL (1992).

[11] G.L. Jackson et al., J. Nucl. Mat. **266-269** (1999) 380.

[12] W.R. Wampler, D.G. Whyte, C.P.C. Wong et al., "Suppression of net erosion in the DIII–D divertor with detached plasma," J. Nucl. Mat., **290-293** (2001)346-351.

[13] W.R. Wampler, D.G. Whyte, C.P.C. Wong, "Erosion in the DIII–D divertor by neon-detached plasma," J. Nucl. Mat., **313-316** (2003) 333-336.

[14] D.G. Whyte, W.P. West, C.P.C. Wong et al., "The effect of detachment on carbon divertor erosion/redeposition in the DIII–D tokamak," Nucl. Fusion, Vol. **41,** No. 9 (2001) 1243-1252.

[15] D.G. Whyte, W.P.West, R. Doerner et al., "Reduction of divertor carbon sources in DIII–D," J. Nucl. Mat., **290-293** (2001)356-361.

[16] G.H. Matthews, P.C. Stangeby, P.C. Elder, J.D. Gottardi et al., J. Nucl. Mat. **196-198** (1992) 374.

[17] J.A. Boedo, D.L. Rudakov, R.J. Colchin et al., "Intermittent convection in the boundary of DIII–D," J. Nucl. Mat. **313-316** (2003) 813-819.

[18] D.G. Whyte, J.P. Coad, P. Franzen et al., "Similarities in divertor erosion/redeposition and deuterium retention patterns between the tokamaks ASDEX Upgrade, DIII–D and JET," Nucl. Fusion, Vol. **39**, No. 8, 1999.

[19] W.P. West, G.D. Porter, T.E. Evans, "Modeling of carbon transport in the divertor and SOL of DIII–D during high performance plasma operation," J. Nucl. Mat., **290-293** (2001)783-787.

[20] R. Bastasz, W.R. Wampler, J.A. Whaley, D.G. Whyte, P.B. Parks, N.H. Brooks, W.P. West and C.P.C. Wong, "Characterization of Energetic Deuterium Striking the Divertor of the DIII–D tokamak," J. Nucl. Mat. 241-243 (1997) 650-654.

[21] P.B. Parks, R. Bastasz and D. Whyte et al., "First Measurements of the Ion Energy Distribution a the Divertor Strike Point During DIII–D Disruptions," 16th SOFE conference, U. of Illinois, 1995, 821-824.

[22] C.P.C. Wong, R.J. Bastasz, D.G. Whyte et al., "Erosion Results from DiMES and Design Implications to ITER and STARLITE," 12th Topical Meeting on the Technology of Fusion Energy, June 16-20, Reno, Nevada, 1996, 694-698.

[23] G. Federici, C.H. Skinner, J.N. Brooks et al., "Plasma-material interactions in current tokamaks and their implications for next step fusion reactors," Nucl. Fusion, **41** (2001) 1967-2137.

[24] T.Q. Hua, J.N. Brooks, "Erosion/redeposition analysis of the DIII–D divertor," J. Nucl. Mat., **220-222** (1995) 342-346.

[25] M. Abdou and the APEX Team, "Exploring novel high power density concepts for attractive fusion systems", Fusion Engineering & Design, **45**, No.1: 145-167 (1999).

[26] J.P. Allain, D.G. Whyte, J.N. Brooks, "Lithium erosion experiments and modeling under quiescent plasma conditions in DIII–D," to be published, 2003.

[27] D.G. Whyte, T.E. Evans, C.P.C. Wong et al.," "Experimental observations of lithium as a plasma-facing surface in the DIII–D tokamak device," submitted to Fusion Engineering and Design, 2003.

[28] N. Yoshida, M. Miyamoto, K. Tokunaga et al., "Microscopic damage of metals exposed to the helium discharges in TRIAM-1M tokamak and its impact on hydrogen recycling process," Nucl. Fusion, **43** (2003)655-659.

[29] M.Y. Ye, H. Kanehara, S. Fukuta et al., "Blister formation on tungsten surface under low energy and high flux hydrogen plasma irradiation in NAGDIS-I," J. Nucl. Mat. **313-316** (2003)72-76.

[30] "A plan for the development of fusion energy," final report to FESAC, March 5, 2003.